Analysis of shared synaptic inputs to different motor unit subgroups in triceps surae during a postural standing task

american physiological society | JNP JOURNAL OF NEUROPHYSIOLOGY

J Neurophysiol 134: 1007–1019, 2025.
First published August 19, 2025; doi:10.1152/jn.00508.2024

RESEARCH ARTICLE

Control of Movement

Analysis of shared synaptic inputs to different motor unit subgroups in triceps surae during a postural standing task

Joshua W. Cohen,[1,3] Taian Vieira,[5] Tanya D. Ivanova,[2] and S. Jayne Garland[2,4]

[1]*School of Kinesiology, Western University, London, Ontario, Canada;* [2]*Physical Therapy, Faculty of Health Sciences, Western University, London, Ontario, Canada;* [3]*Collaborative Specialization in Musculoskeletal Health Research, Bone and Joint Institute, Western University, London, Ontario, Canada;* [4]*Department of Physiology and Pharmacology, Schulich School of Medicine & Dentistry, Western University, London, Ontario, Canada; and* [5]*Laboratorio di Ingegneria del Sistema Neuromuscolare (LISiN), Dipartimento di Elettronica e Telecomunicazioni, Politecnico di Torino, Turin, Italy*

Abstract

Previously, we have observed differential firing behaviors and recruitment locations of distinct motor unit (MU) subgroups within the same muscles. This study examined the amount of shared synaptic inputs to these MU subgroups. Twenty-four participants (10 healthy young adults: 5 females, 5 males; means ± SD: age 27 ± 2.5 yr and 14 healthy older adults: 6 males and 8 females; means ± SD: age 74.8 ± 5.3 yr) stood on a force platform and leaned in five directions maintaining their center of pressure for 35 s per direction. High-density surface electromyography recordings from the medial gastrocnemius, lateral gastrocnemius, and soleus were decomposed into single MU action potentials. MU tracking classified MUs as "common" or "unique" across leaning directions. Synaptic input was estimated using a coherence analysis (proportion of common input; PCI). Three PCI analyses (common, unique, and between the MU subgroups) quantified neural connectivity. MU subgroup significantly affected PCI ($F = 25.92$, $P < 0.0001$), with common MUs exhibiting higher PCI than unique (MD = 0.08, CI [0.07, 0.09], $P < 0.0001$) and between-subgroup MUs (MD = 0.04, CI [0.03, 0.05], $P = 0.0058$). Unique MUs had significantly lower PCI than between-subgroup MUs (MD = 0.04, CI [0.03, 0.06], $P = 0.048$). Taken together, both subgroups receive shared neural inputs for task-specific force production, more so in the common motor units. Importantly, a main effect of age ($F = 4.56$, $P = 0.04$) was observed, with older adults exhibiting higher PCI, though post hoc analyses did not reveal significant differences ($P = 0.45$–0.67).

NEW & NOTEWORTHY Our study reveals differing amounts of shared neural inputs to MU subgroups within the same muscle during standing balance. The proportion of common input (PCI) varies with leaning direction, indicating task dependency and different descending and proprioceptive inputs. Surprisingly, age did not significantly affect PCI values in any MU subgroup or the entire muscle, suggesting that age-related differences in recruitment and firing patterns are more related to factors such as proprioceptive feedback than a common input.

aging; motor units; neural mechanisms; postural control; proportion of common input

INTRODUCTION

The motor control of maintaining upright posture has been investigated extensively over the past 30 years. For instance, muscle synergies have been suggested as a means to address the degrees of freedom problem (1, 2). These muscle synergies are thought to be controlled by a single neural command, which thereby would decrease the degrees of freedom. It has been shown that the vertebrate and invertebrate nervous systems use flexible combinations of muscle synergies to produce a wide range of motor behaviors (3–8). However, recent studies have demonstrated that synergistic muscles may be controlled by separate synaptic inputs (9–11).

To estimate the amount of common synaptic input, researchers have calculated the coherence of the firing patterns between motor neurons within the same muscle. Most of the literature on coherence of agonistic muscles and their synergists has determined a high level of common drive to

Correspondence: S. J. Garland (jgarland@uwo.ca).
Submitted 29 October 2024 / Revised 24 November 2024 / Accepted 10 August 2025

the muscles (12–15). Common drive refers to the correlated neural signals driving MUs (MUs), which can originate from descending pathways, afferent feedback, or interneurons. In contrast, newer analyses [e.g., proportion of common input (PCI)] parameterize these coherence patterns to estimate the proportion of shared synaptic input quantitatively. Although common drive provides insight into the timing of correlated activity, PCI advances this by quantifying the extent of shared input across pairs of MUs. PCI has been used in various isometric conditions (16, 17), however, to our knowledge it has not been applied to postural control research to determine shared input across MU groups.

Our research group used high-density surface electromyography (HDsEMG) to observe differential behavior of distinct MU subgroups within the motoneuron pool of the triceps surae in both young and older adults (18–20). Specifically, during a postural control task of leaning in different directions, we found that there are distinct MU subgroups (common and unique) that behave differently. Common units were defined as MUs that were present across different leaning directions, whereas unique units were MUs that could not be matched across leaning directions. We observed that common MUs were recruited in similar muscle locations during each leaning direction and suggested that they served to establish a baseline level of force production. MUs that were unique to a single leaning direction were surmised to be recruited based on a mechanically advantageous location within the muscle in relation to the force direction of the task (18). These unique units also had higher firing rates than common MUs (19). This pattern of regional recruitment and differential firing behavior of the MU subgroups was observed to be diminished in older adults (20) and may possibly explain conflicting coherence results previously found comparing young with older adults (21, 22).

The mechanisms underlying this differential recruitment and firing pattern are unclear. There are two main hypotheses that may explain our previous observations. First, the recruitment and firing patterns of common and unique units could be modulated based exclusively on their size. This would imply that both populations share the same synaptic input. If this were the case, we would not expect to observe unique units in all leaning directions, but only for the direction imposing the greatest force demand. On the other hand, if we hypothesize that unique and common units receive different amounts of shared synaptic input and belong to distinct pools, the distinct control signals may underlie the differential behavior and regional recruitment that is observed.

Accordingly, the purpose of this study was to determine the amount of shared synaptic inputs to the distinct MU subgroups (common and unique units) within the triceps surae. In addition, we assessed whether older adults had differences in the distribution of synaptic inputs compared with young adults. Based on our prior findings that distinct MU subgroups (common vs. unique units) exhibit different recruitment patterns during postural tasks (18–20), we hypothesized that the amount of shared synaptic input within the unique MU subgroups would be lower than that within the common MU subgroups. This hypothesis stems from the notion that unique MUs are likely driven by more independent neural inputs due to their distinct recruitment during specific task conditions (leaning directions), whereas common MUs, which are recruited across multiple directions, likely receive a greater amount of shared synaptic input (9, 23). Furthermore, given prior research indicating that aging can affect MU behavior, particularly in terms of neural drive and proprioceptive feedback (21, 24), we hypothesized that older adults would exhibit lower levels of shared synaptic input compared with younger adults. It is important to note that lower levels of shared synaptic input do not necessarily imply more independent control. Shared synaptic inputs reflect the degree of commonality in neural drive among MUs, but reductions in shared input may also result from increased noise, changes in MU recruitment strategies, or declines in the precision of descending or afferent pathways (25). The current study will address these questions through a secondary analysis of previous work (18–20). Unlike our earlier work, which primarily focused on MU recruitment patterns and firing behaviors, this study leverages PCI analyses, an innovative application in postural control research, to quantify the extent of neural connectivity within and between MU subgroups.

METHODS

Participants and Experimental Protocol

As previously mentioned, this study is a secondary analysis of three previous studies (18–20). Many details outlining the experimental protocol, decomposition, and tracking can be found there.

Thirty-one participants were recruited for these studies, however, only 24 participants were included in this analysis (see *Proportion of Common Input and Cumulative Spike Train Coherence* for details): 10 healthy young adults between 19 and 40 yr of age (5 females, 5 males, means ± SD: age 27 ± 2.5 yr; body mass 68.2 ± 12.3 kg; height 173.6 ± 4.3 cm), and 14 healthy older adults over the age of 69 yr (6 males and 8 females, means ± SD: age 74.8 ± 5.3 yr, body mass 75.4 ± 15.3 kg; height 171.8 ± 12.2 cm).

Informed written and verbal consent was acquired from each participant. Exclusion criteria were the presence of comorbidities (neuromuscular, neurological, balance disorders, etc.) or lower limb injuries within the past 6 mo. The study conformed to the standards established by the Declaration of Helsinki, latest amendment, and was approved by the Institutional Ethics Committee (Research Ethics Board Number: 110471).

Experimental Protocol

The experimental data in this study were derived from a broader investigation into the spatial characteristics of motor unit (MU) recruitment (18–20). Participants stood naturally on a piezoelectric force platform (9286AA Kistler, Zurich, Switzerland) and were instructed to lean in various directions. To determine the limits of stability (LoS), participants leaned at the ankles in anterior, posterior, and lateral directions as far as possible without stepping. This four-directional LoS assessment has been demonstrated to be more reliable for evaluating stability limits compared with other tests (26).

Following the LoS test, participants completed a 30-s quiet stance trial. The recorded center of pressure (CoP) in this

first trial was used to determine target locations for visual feedback in subsequent leaning tasks (Fig. 1*A*). Participants were then asked to lean toward targets positioned at 0°, 30°, 60°, 90°, and 120°, measured counterclockwise from the mediolateral axis intersecting the average CoP position during the quiet stance. Each target was displayed individually on a screen positioned in front of the participant (Fig. 1, *A* and *B*). These targets appeared over an elliptical region with semi-axes set at either 30% or 40% of the LoS in the anterior-posterior and mediolateral directions (Fig. 1*B*). Progressively higher contraction intensities were required for the targets at 80% of LoS (compared with 60%) due to the proportional relationship between the CoP distance and ankle torque (27).

Participants leaned toward each target, held their CoP within the target area for 35 s, and then returned to the quiet stance position. The 35-s duration was a sufficiently long time window to reliably conduct PCI analysis (see *Proportion of Common Input and Cumulative Spike Train Coherence*) and to provide an adequately difficult task to elicit appropriate postural responses. A 15-s rest period was provided after each leaning task. The CoP trace for the leaning task is illustrated in Fig. 1*C*. During the leaning, participants were instructed to maintain a straight body posture, moving like a rigid pole. Movements were performed smoothly, with a total trial duration of 45 s (5 s moving toward the target, 35 s holding in position, and 5 s returning to stance). This provided an isometric-like contraction to allow for decomposition of EMG signals. Small changes in muscle lengths were possible; however, they would not be expected to exceed the maximal (250 μm: mean + 3 SD) change in muscle length reported during quiet standing (28).

Before the recorded trials, participants completed a practice session to familiarize themselves with the task. Trials were discarded and repeated if participants did not maintain the specified posture or if they were unable to stabilize their CoP in the target for at least 25 s. Trials were retained for analysis once the appropriate posture and CoP stability were achieved.

High-Density Surface EMG Placement and Collection

EMG placement was guided using an ultrasound imaging system (LogicScan 64 LT-1T; Telemed, Vilnius, Lithuania). Surface EMG signals were recorded from the medial gastrocnemius (MG) and lateral gastrocnemius (LG) using a 32-channel high-density surface EMG (HDsEMG) grids. Each grid consists of 8 × 4 electrodes (1-mm diameter, 10-mm interelectrode distance). The grids were placed 10 mm above the distal edges of the superficial aponeurosis of the MG and LG. Surface EMG signals were recorded from the soleus (SOL) using a 64-channel HDsEMG grid (8 × 8 electrodes, 1-mm diameter, 10-mm interelectrode distance). The SOL grid was centered over the Achilles tendon, 10 mm below the distal insertion of the MG. Bioadhesive foam held the grids in place, and conductive paste was used to ensure optimal electrode skin contact. Three reference electrodes were placed on the patella, the fibular head, and the medial malleolus for MG, LG, and SOL, respectively. HDsEMG signals were collected in monopolar configuration. Signals were amplified 500 times using a multichannel amplifier (128-channel EMG-USB with OTBioLab software v.2.05; OTBioelectronica, Torino, Italy) and digitized at 2,048 Hz using a 12-bit analog to digital converter.

Force Plate Recordings

CoP coordinates in the sagittal and frontal planes were computed from the ground reaction forces, sampled at 2,048 Hz using a separate 16-bit A/D converter (NI 9205, National Instruments Co, Austin, TX) and an interface to MATLAB

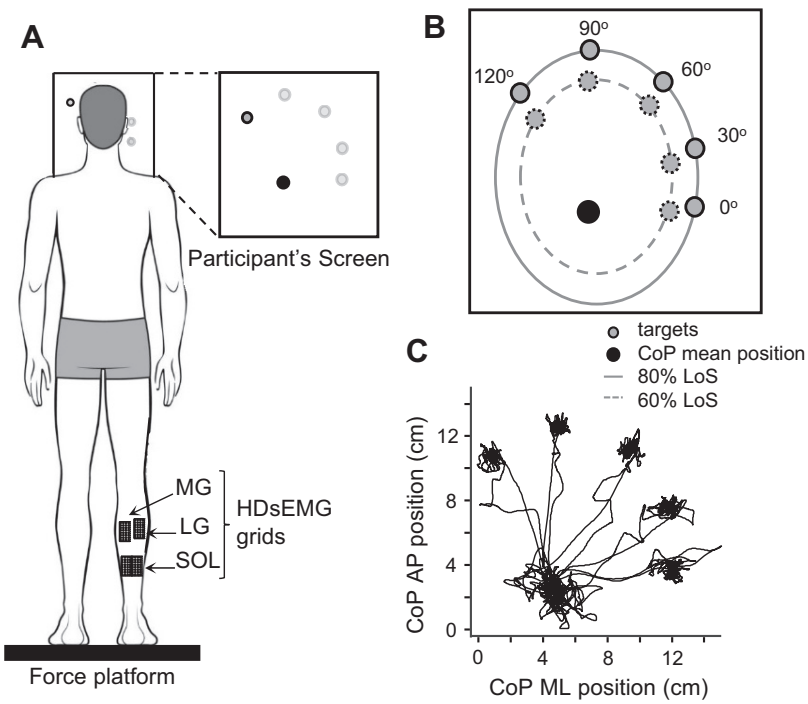

Figure 1. Experimental set up. Schematic of the experimental setup for the multidirectional leaning task. *A*: a participant stands on a force platform, monitoring their center of pressure (CoP) movements in real-time as they lean toward the specified targets. *B*: the screen displays the participant's CoP, the leaning targets, and the 60% (dashed line) and 80% (solid line) limits of stability (LoS). The five leaning directions (0°, 30°, 60°, 90°, and 120°) are represented by gray circles, positioned along ellipses derived from the participant's LoS measurements. Only one target was shown at a time during the task. High-density surface electromyography (HDsEMG) sensors were placed over the medial (MG) and lateral (LG) gastrocnemius and the soleus (SOL). *C*: example of the center of pressure (CoP) trace from a single participant during the multidirectional leaning task. AP, antero-posterior; ML, mediolateral.

2020 b (The MathWorks, Inc., Natick, MA) that displayed the targets and the real-time position of the CoP. The force signals were recorded simultaneously by the EMG system to synchronize both systems.

Data Analysis

MU decomposition.

All EMG analyses were performed using MATLAB 2024a. From the monopolar signals, single differential EMGs were calculated between pairs of adjacent electrodes along each column of the matrix. Visual inspection was completed for quality, and channels presenting contact problems or power line interference were linearly interpolated. After that, monopolar signals were filtered (Butterworth, 2nd order, 20–350 Hz) and decomposed using the blind source separation method (29, 30) implemented in the DEMUSE tool software. The decomposition was conducted for each target direction and LoS condition separately, over the central 20 s of the 35 s period when the CoP was maintained at the target location. The single differential EMGs computed along the columns of the grid were averaged over 30-ms epochs using the firing instants of identified MUs as a trigger, providing the surface representation of single MU action potentials (Fig. 2). The results of the decomposition were inspected visually for spurious units. No manual editing of spike trains was performed in this study but MUs with propagating potentials, noisy waveforms, and those with a pulse-to-noise ratio below 28 dB were discarded (30, 31).

MU tracking.

A MU tracking analysis was conducted separately for the 60% and 80% LoS conditions. MU action potentials that were common between the different leaning directions were identified by focusing on both the shape and amplitude of the MU action potential waveforms. For each retained MU, the average rectified value (ARV) was calculated across 30-ms epochs centered on individual action potentials. Each retained MU was paired to all other MUs identified during different leaning directions within the same muscle and LoS condition for each participant (e.g., an MU identified in the 0° leaning direction in the 60% LoS condition within the MG is compared with all other units identified in the MG at the 30°, 60°, 90°, and 120° leaning directions of the 60% LoS condition within a single participant). The action potentials for each pair of MUs were aligned in time by maximizing their cross-correlation function. The mean square difference was calculated between the two sets of time-aligned action potentials, averaged across channels, and then normalized with respect to the mean ARV of the two sets of action potentials. This normalization procedure is used to reduce the bias of waveform amplitude between two MU pairs (32). Finally, pairs of MU action potentials with a mean square difference smaller than 10% were considered common (18, 33). An expert operator visually confirmed all MUs that were identified as common by the algorithm. This provided us with a group of MUs that will be referred to as common units that were present in two leaning

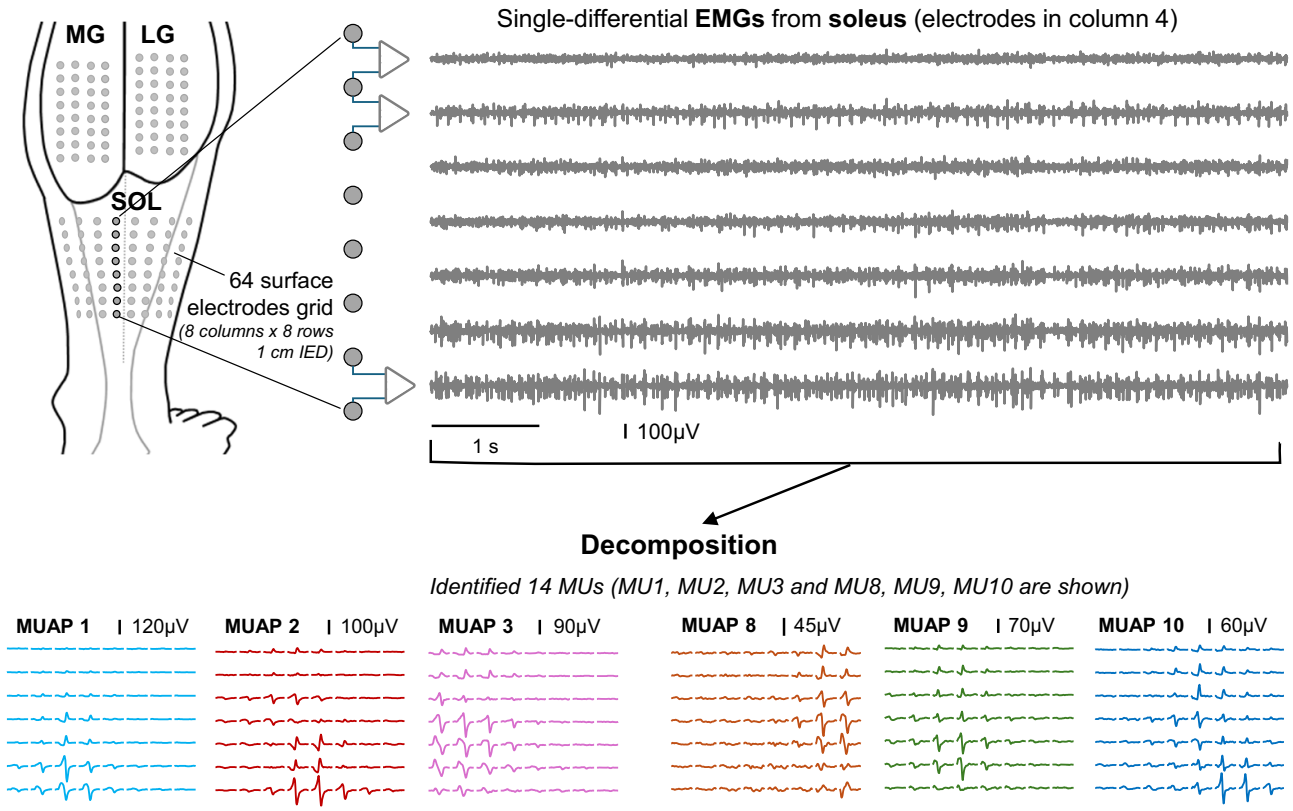

Figure 2. Spatial representation of MUs. Examples of MU action potentials (*bottom*) decomposed from the soleus muscle's high-density surface electromyography (HDsEMG) signals. Presented are the positions of the HDsEMG sensors (*top left*) placed over the medial (MG) and lateral (LG) gastrocnemius (two 32-electrode grids) and the soleus (SOL; one 64-electrode grid), together with a 10-s sample (*top right*) of single differential EMG from column 4 of the SOL grid. MU, motor unit; SOL, soleus.

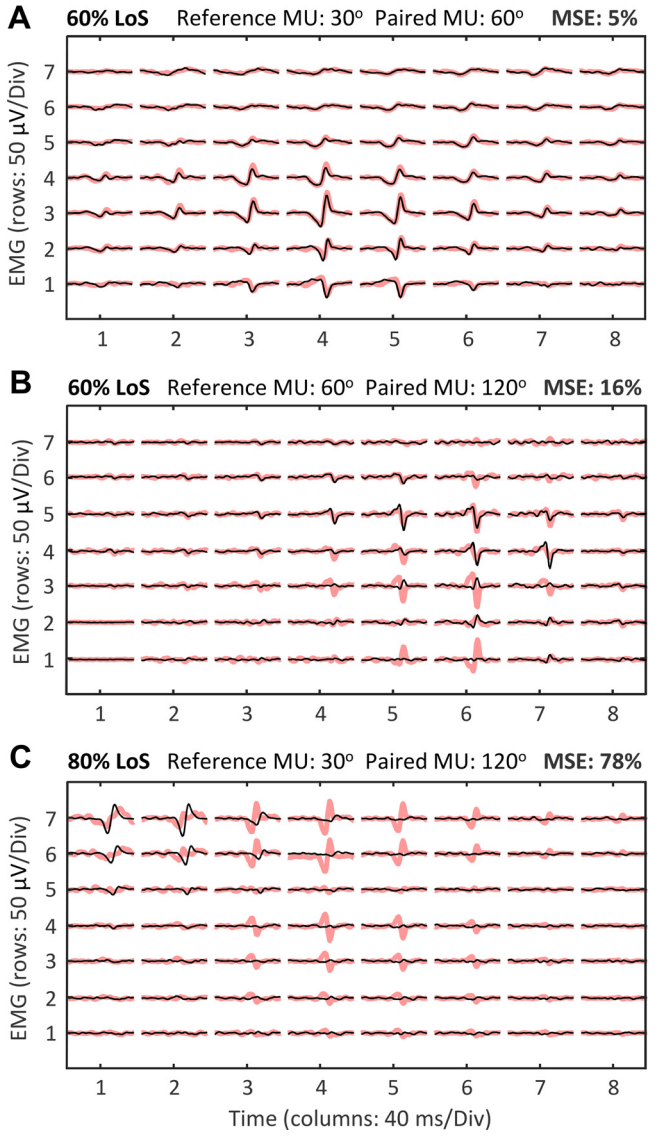

Figure 3. Example of MU matching ($N = 6$ MUs). Illustration of MU pairs that were matched (*A*) and two MU (MU) pairs that were not matched (*B* and *C*). The reference MU is shown in red, and the paired MU in black. *A*: an example of an MU considered common, with a mean square error (MSE) of 5%. *B* and *C*: examples of MU pairs considered unique, with MSE values close to the 10% threshold (*B*: MSE = 16%) and well above it (*C*: MSE = 78%). The vertical and horizontal axes represent the channel row and column numbers from the high-density surface electromyography, respectively. LoS, limit of stability. MU, motor unit.

conditions or more. When a MU had a mean square difference greater than 10% with all MUs it was paired with, the MU was considered to be a uniquely recruited unit not found in other leaning directions. These MUs will be called unique units from this point. (See Fig. 3).

Proportion of Common Input and Cumulative Spike Train Coherence

To calculate the amount of shared synaptic input to the MUs, we conducted a form of coherence analysis proposed by Negro et al. (16) called the proportion of common input (PCI). The PCI is derived from the relationship between the average coherence and the number of motoneurons used to determine it. The general steps of the PCI calculation are outlined below and in Fig. 4.

Step 1 (Grouping MUs): The MUs used for PCI analysis are divided into two groups with an equal number. Coherence is computed between cumulative spike trains (CSTs) with an increasing number of spike trains. All combinations of MUs within and between the two groups are considered for constructing the CSTs, with the number of MU spike trains from each group varying from one to half of the number of analyzed units.

Step 2 (Cumulative spike trains): For each MU, the spike train was defined as a vector with 40,960 samples (2,048 Hz $\times$ 20 s) where at each time point (sample), the data are either 0 (no firing) or 1 (firing). Cumulative spike trains (CSTs) were generated by summing the individual spike trains of the MUs selected from each group for each combination of MUs. When only one unit from each group is considered, the CST is the firing pattern of the corresponding unit.

Step 3 (Coherence calculation): The normalized coherence was then computed between the CSTs representing the selected MUs. Nonoverlapping epochs of 1s, zero-padded to 5 s (0.2-Hz frequency spacing) without tapering, were considered for computing coherence between CSTs. Normalized coherence values range from 0 to 1, respectively, indicating no correlation and perfect correlation between CSTs for each frequency. This approach ensures that coherence remains invariant to the amount of change in discharge characteristics (e.g., discharge rate, coefficient of variation of the interspike interval), providing information regarding the source of the synaptic inputs driving these behaviors.

Step 4 (Parameterization of coherence): The coherence calculation was parameterized to obtain the mean coherence within the specified frequency band (0–5 Hz). This low-frequency band (delta band) has been demonstrated to be the frequency in which movement is most directly associated with force generation (34) and is most associated with common drive (35–37). Mean coherence (over 0–5 Hz) computed between CSTs with the same number of spike trains was averaged across all MU combinations.

Step 5 (Fitting experimental coherence data): The coherence data, collected for CSTs created from varying numbers of motor neuron spike trains and averaged over the 0–5-Hz frequency band, were fitted using nonlinear least-square solvers (using the MATLAB *lsqcurvefit* function) to estimate the square root of the ratio A/B (16). The parameters A and B correspond to the power of the common synaptic input and the response of the motor neuron pool to independent synaptic inputs for the unique and common units.

Step 6 (PCI estimation): The square root of the ratio A/B is referred to as the PCI. The resulting PCI serves as a quantitative measure, estimating the proportion of common synaptic input shared between the MU comparison groups. This comprehensive analysis provides an estimation of the shared synaptic input underlying the firing behaviors of the MU subgroups. For further details on the methodology, refer to the original paper by Negro et al. (16) and corresponding figures, tables, and derivations.

Specifically for the current study, the number of MUs per group for *step 1* of the analysis was a minimum of four and a maximum of seven MUs (half of the maximum number of MUs analyzed). The number of MU pairs at times was

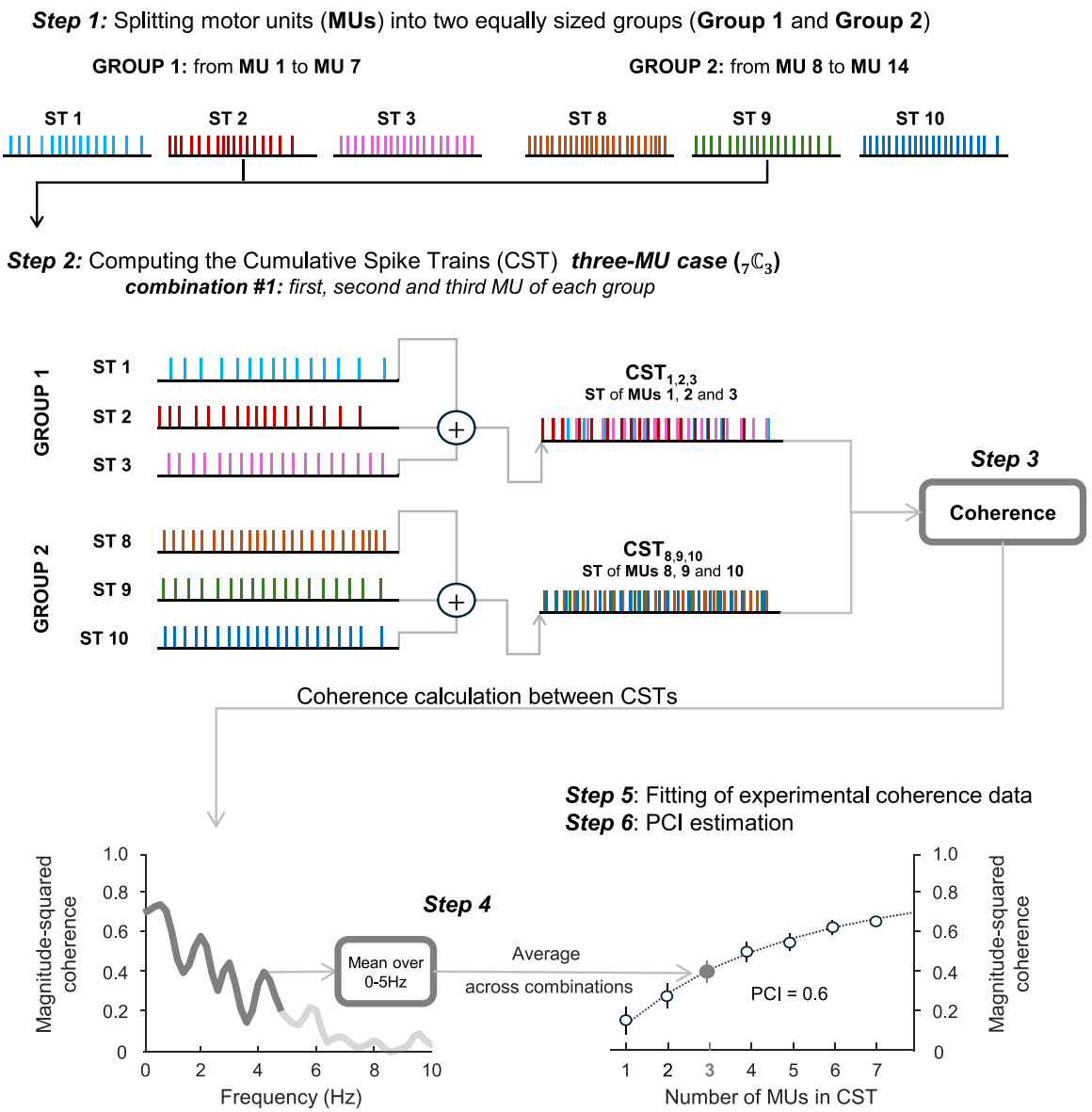

Figure 4. Visual representation of cumulative spike train and proportion of common input analysis ($N = 14$ MUs). Example of step-by-step proportion of common input (PCI) calculation for 14 MUs (MUs) from the same muscle (only the first 6 MUs are shown). These MUs are spatially represented in Fig. 2 (according to colour). Step 1: grouping MUs into two equally sized groups. Step 2: generation of cumulative spike trains (CSTs) by summing individual spike trains of selected MUs for one of the MU combinations. Step 3: coherence calculation between CSTs (light gray line) for nonoverlapping epochs of 1 s. Step 4: parameterization of coherence within the 0–5-Hz frequency band (dark gray line), associated with movement and force generation. Mean coherence values over 0–5-Hz band are averaged across all combinations of MUs. Step 5: fitting experimental coherence data using nonlinear least-square solvers to estimate the square root of the ratio A/B [from *Eq. 4*, Negro et al. (16, 23)]. Step 6: PCI estimation, derived from the square root of A/B ratio, provides a quantitative measure of shared synaptic input. Refer to Negro et al. (16, 23) for detailed methodology. CST, cumulative spike train; MU, motor unit; PCI, proportion of common input.

different for each direction within a participant due to differing decomposition yields. To reduce bias in the coherence calculations, we used the minimum number of MU pairs collected from a single participant within a direction (4 MU pairs) to calculate the PCI. If we were unable to decompose at least eight MUs per muscle and leaning direction, the participant was excluded from analysis. Seven participants were excluded from analysis for this reason.

Using the above steps, we conducted three separate PCI analyses to assess the amount of shared synaptic input provided within each MU subgroup and between the MU subgroups. Two PCI analyses were conducted within each of the distinct motoneuron subgroups (i.e., a unique unit analysis and a common unit analysis). A third PCI analysis was conducted to assess the amount of shared synaptic input between the two MU subgroups (i.e., a unique and common unit analysis). For this PCI analysis, referred to as "between MU subgroups" or "PCI between MU subgroups" elsewhere in the text, groups 1 and 2 in *step 1* consisted of all MUs from both MU subgroups. The three PCI analyses enabled us to determine whether there was shared synaptic input within MUs of each subgroup, and whether there was overlapping

synaptic input to both MU subgroups, directly addressing our research question of whether there are separate and/or shared synaptic inputs to the distinct MU subgroups. See Fig. 4 for a visual representation of the PCI analysis. These analyses were performed for each participant, leaning direction, muscle, and LoS separately.

The number of LG MUs that were decomposed per person was too low to conduct the PCI calculations. Thus, the PCI analysis was only performed for the MG and SOL muscles. The PCI with respect to the total input received by the motor neuron pool was estimated from the average values of coherence in the delta bandwidth (0–5 Hz) and the number of MUs used in the calculation. In the PCI calculation, as the number of MU pairs increases, so do the coherence values (16).

Statistical Analysis

All statistical analyses were conducted using R (v.5.12.1, R Development Core Team, 2009). To determine if the PCI value was influenced by the motor unit discharge rate, we correlated the PCI with the average discharge rate for unique and common motor units separately for MG and SOL. There was no significant effect of discharge rate on the PCI, with low R^2 values (less than 2% of variance explained by the association).

The effect of the independent variables, MU subgroup (common, unique and both common and unique MUs), muscle (MG and SOL), leaning direction (0°, 30°, 60°, 90°, and 120°), LoS (60% and 80%), and age (young and older adults), on PCI was determined using a single linear-mixed model.

Model specification.

The initial model included all predictors and their interactions, with a maximal random structure:

$$\begin{aligned}\text{initial\_model} < -\text{lmer}(\text{PCI} \sim \text{MU\_subgroup} \times \text{muscle} \\ \times \text{leaning\_direction} \times \text{LoS} \times \text{Age} \\ + (1 + \text{leaning\_direction} + \text{muscle} \\ + \text{MU\_subgroup} + \text{LoS} \,|\, \text{subject})\end{aligned}$$

Model construction.

We started with the maximal random structure, including by-participant random intercepts and slopes for all predictors. However, due to collinearity and convergence issues (identified through singularities and convergence diagnostics), we simplified the random effects structure. The optimal random structure retained random intercepts for participants and random slopes for leaning direction and muscle:

$$\begin{aligned}\text{optimal\_model} < -\text{lmer}(\text{PCI} \sim \text{MU\_subgroup} \times \text{muscle} \\ \times \text{leaning\_direction} \times \text{LoS} \times \text{Age} \\ + (1 + \text{leaning\_direction} + \text{muscle} \,|\, \text{subject})\end{aligned}$$

We did not include random slopes for LoS and MU subgroups due to collinearity issues. Model simplification was guided by likelihood ratio tests, comparing models with progressively reduced random structures to identify the optimal model.

Statistical testing.

Statistical significance of fixed effects was assessed using type III Wald F tests with Kenward–Roger degrees of freedom via the anova() function from the car package (v. 3.0.12).

Post hoc testing.

Post hoc pairwise comparisons were conducted using the emmeans package (v. 1.7.2) with Bonferroni's correction applied to account for multiple comparisons. These tests were performed on the main effects of the fixed factors, consistent with the overall model structure. We did not perform post hoc tests on interactions as the final model did not include interaction terms. Post hoc comparisons were made between target direction and within the same target direction for the LoS condition, muscle group, and MU subgroup. The number of tests included in the Bonferroni correction was determined by the total number of pairwise comparisons performed.

Confidence intervals.

Confidence intervals (95%) for the parameter estimates were calculated via parametric bootstrapping with 5,000 iterations. However, we recognize the redundancy in reporting both bootstrap confidence intervals and P values from the emmeans comparisons. To avoid confusion, we report only the P values and confidence intervals derived from the emmeans comparisons.

RESULTS

The total number of MUs decomposed for the 24 participants was 4,336 (MG: 2,240, SOL: 2,096). Due to using the minimum number of MU pairs for the coherence analysis to eliminate bias, the total number of assessed MUs was 3,840 (8 MUs, in 5 leaning directions, during 2 LoS conditions, in 2 muscles for 24 participants).

Proportion of Common Input

There was a statistically significant main effect of the MU subgroup ($F = 25.92$, $P < 0.0001$) on the PCI values, with higher PCI in the common units compared with the unique units (MD = 0.08, CI [0.07, 0.09], $P < 0.0001$) and the PCI between the MU subgroups (MD = 0.04, CI [0.03, 0.05], $P = 0.0058$) (Fig. 5). In addition, the PCI estimated between the MU subgroups was higher than for the unique units (MD = 0.04, CI [0.03, 0.06], $P = 0.048$) (Fig. 5).

There was no main effect of LoS on the PCI ($F = 1.42$, $P = 0.23$). However, there was a main effect of muscle ($F = 231.44$, $P < 0.0001$), with higher PCI for the MG compared with the SOL, on average across the MU subgroups, directions, LoS levels, and age groups (MD = 0.127, CI [0.119, 0.135], $P < 0.0001$) (Fig. 5).

There was a statistically significant effect of the leaning direction ($F = 11.12$, $P < 0.0001$) on average across the MU subgroups, muscles, LoS levels, and age groups, with lower PCI during the 30° (MD = 0.055, CI [0.042, 0.067], $P = 0.01$), 60° (MD = 0.052, CI [0.049, 0.55], $P = 0.01$), and 90° (MD = 0.078, CI [0.065, 0.091], $P = 0.01$) leaning directions compared with the 0° leaning direction (Fig. 5). Although all pairwise comparisons were performed, only significant comparisons to the 0° direction are reported here for brevity.

There was a main effect of age ($F = 4.56$, $P = 0.04$), indicating that older adults had higher PCI values compared with younger adults. However, the post hoc analysis did not show significant differences after applying Bonferroni correction (post hoc P values ranging from 0.45 to 0.67). Thus,

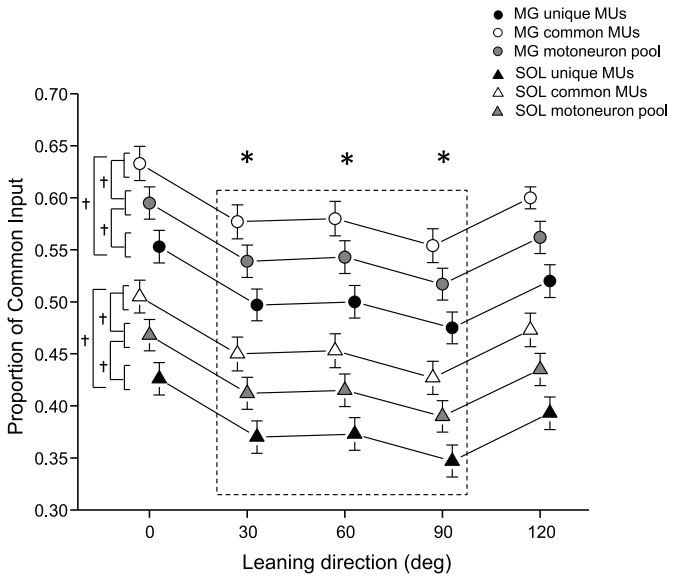

Figure 5. Estimated means of the PCI linear mixed-model analysis (N = 3,840 MUs). Proportion of common input for the three separate MU subgroups (black: unique; white: common and gray: between the MU subgroups) in the MG (circles) and SOL (triangles). The estimates are calculated from the linear mixed model, with participants as random intercepts, and fixed effects of MU subgroup analysis, leaning direction, muscle, LoS, and age. The PCI was significantly higher in the common units compared with the unique units, and compared with the between MU subgroup analysis. The PCI was significantly higher in the between MU subgroup analysis, compared with the unique units. There was a muscle effect with the MG having higher PCI compared with the SOL in all conditions. Finally, there was a directional effect with a decrease in PCI at the 30°, 60°, and 90° leaning direction, suggesting a task/directional dependency of the PCI values. *Significantly different between leaning directions ($P < 0.001$). †Significantly different between MU subgroups ($P < 0.001$). MG, medial gastrocnemius; MU, motor unit; PCI, proportion of common input; SOL, soleus.

the main effect of age indicates an overall pattern, but the Bonferroni-corrected post hoc tests do not support strong age-related differences in specific comparisons.

DISCUSSION

The main findings of this secondary analysis reveal that the amount of shared neural inputs to distinct subgroups of MUs within the same muscle during standing balance varied by subgroup. That is, the PCI values for the common units were higher compared with the unique units across all directions, indicating that more shared neural inputs were sent to the common MU subgroup. However, the PCI between MU subgroups was higher than the unique units alone and lower than the common units alone, indicating a different degree of shared neural input to the subgroups. In addition, the PCI appears to exhibit task dependency, with the highest PCI observed during the 0° direction, and the lowest during the 90° direction.

Shared Synaptic Inputs of MU Subgroups

It has been previously proposed that volitional force modulation is partially determined by common inputs sent to motor neurons, which results in common fluctuations in the discharges of motor neurons (36–39). However, there have been recent studies that have reported flexible control of motor neurons. For example, Formento et al. (10) demonstrated that over a training period, participants were able to decrease the dimensionality of MU activity (dimensionality defined as the number of independent factors that described the firing rates of the MU) during ramp and hold isometric contractions. This ability to decrease the dimensionality illustrates that in the untrained motor system, there are flexible combinations of control present that at some level are controllable. Our current study supports and expands this flexible MU control theory, specifically, during a postural control task. The differing PCI values in response to different leaning directions suggest that the central nervous system (CNS) may provide neural synaptic signals based on force direction.

The results from our previous studies demonstrated that during a postural control task, the CNS regionally recruits distinct MU subgroups (18) that have differential firing behaviors (19, 20) in the triceps surae when leaning in different directions. The addition of the PCI results from this study provide greater information regarding the neural mechanism of these observations. Given that there was a statistically different PCI within the unique and common MU subgroups, and between MU subgroups, it would appear that there are more shared synaptic inputs being sent to the common MU subgroup. Although the common units have the highest amount of common input, there is still an overlap of synaptic input that is similar between the two MU subgroups to control their firing behaviors. This idea of overlapping excitatory commands has been previously described first by Desmedt and Godaux (40) and more recently modified by Hug et al. (11). When Desmedt and Godaux (40) first demonstrated the different MU recruitment orders in response to different movements involving the first dorsal interosseous muscle, they described an overlap of the spinal circuitry between the two motoneuron pools innervating abduction and flexion of the index finger to explain their findings. This organization would allow motor commands to be encoded by movements rather than by muscles as the final path of the motor commands is not strictly common but involves different excitatory connectivities to motoneuron pools responsible for movements in different directions.

Hug et al. (11) described that common inputs do not necessarily project to all motoneurons in a pool but to subpopulations of motoneurons in the entire pool. This framework, advanced by Hug et al. (11), has several hypotheses regarding the consequences of overlapping synaptic input. Our previous studies provide evidence for three of them: *1*) MUs are grouped into functional groups (18, 41); subpopulations may *2*) span across muscles involving only a portion of a muscle, i.e., spatially localized MU subpopulations (18, 20, 41), and *3*) represent functional modules used by the CNS to reduce the dimensionality of the control (18–20).

Applying this framework to our current findings helps explain the mechanisms of distinct and overlapping control. The common units with the highest PCI were recruited in similar locations on the muscles across the leaning directions with lower firing rates (18–20). The unique units, which have the lowest PCI (or the least amount of shared synaptic input), had relatively higher firing rates and were recruited in different locations on the muscle across the leaning directions (18–20). The PCI analysis between MU subgroups revealed moderate

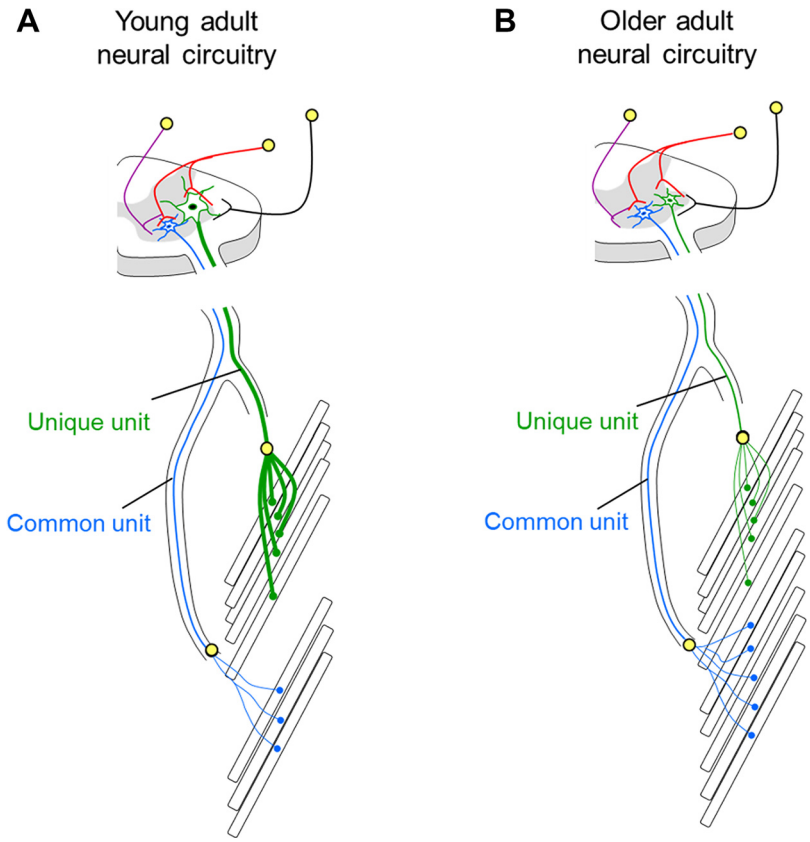

Figure 6. Schematic of neural circuitry in young and older adults controlling unique and common units. Two schematics representing the potential neural circuitry in young adults (*A*) and the associated changes in older adults (*B*). In the young adult, both distinct and overlapping synaptic input is provided to the two motoneuron pools. The common units represented in blue are smaller in size and are likely first recruited to meet force demands. Once the task exceeds the capacity of the common units, unique units (represented in green) can be recruited in distinct locations. Due to the shared excitatory synaptic input, the distinct motoneuron pools may receive similar commands for firing behaviors [e.g., similar modulations in AFR (19, 20)]. However, due to the distinct excitatory synaptic input, different information can still be encoded in the distinct motoneuron pools [e.g., different modulation of CoV_{ISI} (19)]. In the older adult, the common units were larger, putatively due to the denervation-reinnervation process. However, the neural connectivity is likely similar.

PCI values, suggesting shared synaptic input across the motoneuron pool and across leaning directions.

Figure 6 provides a schematic illustration of the spinal circuitry involved in controlling the recruitment of both common and unique MUs in young and older adults. In the young adults (Fig. 6*A*), both distinct and overlapping synaptic inputs are provided to the MU subgroups. The common units, depicted in blue, are smaller and likely recruited first to meet baseline force demands, whereas the unique units, shown in green, are recruited later in specific muscle regions once the force demands exceed the common units' capacity. The figure also shows the potential overlap in synaptic inputs, demonstrating that while these MU subgroups receive distinct inputs, there are shared excitatory inputs that coordinate their firing behavior.

In older adults (Fig. 6*B*), the common units appear larger, potentially due to age-related denervation-reinnervation processes, but the synaptic connectivity is likely similar to that of young adults. Despite age-related changes in MU size, the overlap in excitatory inputs to common and unique units remains, suggesting that the overall organization of synaptic inputs does not differ substantially with age. This schema is intended as a conceptual model illustrating one possible organization of input structure consistent with our findings, and is highlighted as a framework for considering how overlapping and subgroup-specific inputs might contribute to task-dependent motor unit recruitment during postural control tasks.

A critical point to consider when reviewing Fig. 6 is distinguishing proprioceptive feedback and descending drive when interpreting PCI values. PCI values cannot explicitly differentiate the source of synaptic inputs. Instead, PCI quantified the proportion of shared synaptic inputs, regardless of whether that input originates from descending motor commands, spinal interneurons, or afferent proprioceptive pathways. In the context of Fig. 6, it is important to recognize that descending inputs likely provide a top-down control signal, contributing significantly to shared synaptic input, particularly for common MUs. Proprioceptive inputs are modulated based on task requirements and directional demands (42, 43), potentially driving variability in PCI observed between unique MUs recruited for specific leaning directions. The distribution depicted in Fig. 6 reflects the net effect of these sources of synaptic drive, without explicitly distinguishing their relative contribution. Furthermore, the classifications of MU into common and unique subgroups are operationally defined based on the conditions of this specific study. Although common MUs were consistently observed across all directions and unique units appeared only in isolated directions, these classifications are not intrinsic properties of the MU themselves. Rather, they reflect contextual recruitment patterns governed by the demands of this task. As such, delineation may not generalize to other functional contexts and should be viewed as a pragmatic framework for examining differences in synaptic input properties under controlled conditions.

Directionality and PCI

The PCI was influenced by the direction of the leaning task, with the highest PCI for both MU subgroups during the 0°

leaning direction, and the lowest during the 90° condition, demonstrating a task dependency of the shared synaptic input. It has been previously shown that common drive is task dependent, with higher common drive during quiet standing compared with seated volitional isometric contractions (37), suggestive of different descending drive during the postural and voluntary tasks. The lower PCI observed during the 90° leaning direction suggests potential changes in the contribution of descending and proprioceptive inputs to MU pools. Although descending drive reflects top-down control from higher brain centers, proprioceptive feedback provides sensory information from muscle spindles and other sensory organs. These two inputs interact but are distinct in their mechanisms, and their relative contributions to PCI differences across directions warrant further investigation. Although difficult to elucidate the exact origin of the PCI observation, the lower PCI may demonstrate that force demands of the triceps surae are correlated with the PCI.

Lack of Aging Effect

Although our initial hypothesis was that older adults would exhibit reduced shared synaptic input, our results indicate no significant age-related differences in PCI values. This suggests that while age-related changes in proprioceptive feedback are well documented (24), those changes may not significantly alter the shared synaptic drive overserved across MU pools during postural tasks. It is possible that the differences in the older adults' MU firing properties may relate to differences in proprioceptive feedback, rather than common drive.

Previous reports appear to be mixed on the amount of common drive within older adult populations. Semmler et al. (21) found that "within muscle" coherence was higher in older adults than in young adults in the first interosseus muscle. However, aging had no effect on the intermuscular coherence of muscles of the hands (22). To our knowledge, this is the first study to examine PCI of triceps surae MUs in older adults during a postural task. Our results indicate that there is no statistical difference between the PCI of aged and young adults. Perhaps the muscles of the hands and legs have different control schemes. Postural muscles have been shown to behave differently during postural tasks compared with isometric contractions (43–45) and our results indicate that while in some tasks aging leads to higher MU coherence, during postural control, there is no difference compared with young adults.

The lack of statistical significance may also relate to the type of coherence analysis (PCI) and statistical approach used. Classically, researchers have calculated the coherence of the firing patterns between motor neurons by measuring how much the frequency components of two signals are linearly dependent, with emphasis being given to the coherence values in the 0–5-Hz frequency band as this low-frequency bandwidth has been shown to be associated with force output and movement (34). These linear correlational coherence techniques have been used to assess the amount of common drive delivered to a motoneuron pool (35, 36, 46). However, there are several issues with the interpretation of linear correlation measures (39, 47, 48). For example, the measures in the time and frequency domains between pairs of motoneuron spike trains are influenced by the nonlinear nature of the motor neuron discharge (39). In addition, the pairwise correlations of spike trains have high variability, which limits the interpretation of the observations (25). These issues have been extensively reviewed (39) and circumvented with the modeling techniques used in this study (16). By using a phenomenological model of motor neuron activity based on the observation that the summation of multiple spike trains can reproduce the synaptic control signal better with an increasing number of spike trains, the model approximates the absolute proportion of common synaptic input (PCI) delivered to a group of MUs (16). Accordingly, PCI overcomes some of the inherent statistical and nonlinear problems that a linear coherence has. It may be that when these issues are removed, there are no differences in the aging populations. Another advantage is the use of a linear mixed model to assess the differences in PCI between young and older adult populations, as it reduces the bias of within-subject differences. Accounting for this bias, a more robust analysis may be presented in this study.

Technical Considerations

Understanding the neural control of MUs requires careful selection of analytical techniques, each offering distinct insights into the mechanisms underlying MU behavior. In this study, we used PCI to quantify shared synaptic inputs across MU subgroups, particularly in the context of postural control tasks. It is important to note that while PCI offers a quantitative estimate of the proportion of shared synaptic input, it does not directly assess the presence of the structure of independent input sources. Therefore, while differences in PCI values across MU subgroups and conditions suggest variations in input commonality, they should not be interpreted as conclusive evidence for the presence of segregated or orthogonal input streams. Although alternative approaches, such as factor analysis or MU synergy models, have been used effectively in other contexts (11, 49), PCI was selected here for several key methodological considerations.

Strengths and Suitability

PCI provides a quantitative estimate of shared synaptic input to MU subgroups, distinguishing between common and distinct neural drives. This approach is particularly well-suited to address questions about the extent to which different MU subgroups (e.g., common and unique units) are driven by shared neural sources. Traditional measures, such as coherence, capture temporal relationships but do not directly quantify the proportion of shared inputs. PCI advances this understanding by modeling shared variability explicitly. Postural control tasks involve dynamic, direction-dependent demands on MU recruitment and synaptic input patterns. PCI excels in revealing how these task-specific demands shape shared synaptic inputs, an insight that is often less apparent with broader dimensionality-reduction approaches like factor analysis. Traditional metrics (e.g., discharge rate, CoV_{ISI}, intermittency) primarily characterize MU outputs, describing firing behavior patterns without directly addressing the underlying mechanisms driving those patterns. PCI bridges this gap by offering insight into the amount of shared neural inputs received by different

MUs, revealing mechanistic distinctions that would remain obscured with output-focused measures.

PCI is particularly effective when analyzing small, distinct MU subgroups, such as those identified in our study based on their presence ("common") or absence ("unique") across different leaning directions. Factor analysis, in contrast, often aggregates MU behavior across larger groups or modes, which can obscure finer details about subgroup-specific synaptic input patterns. Unlike factor analysis, PCI does not rely on dimensionality-reduction assumptions, such as representing variability across MUs with a small number of principal components. Instead, PCI directly quantifies coherence-derived relationships, minimizing potential oversimplification of neural control strategies.

Comparison with Factor Analysis and MU Synergies

In contrast to PCI analysis, factor analysis excels at identifying overarching patterns of MU synergies and alternative control structures, typically across larger MU groups or multiple muscles (50). Although powerful for reducing data dimensionality and identifying broad organizational modes, factor analysis operates at a different conceptual level, often aggregating MU behavior without isolating subgroup-specific neural inputs. For example, Del Vecchio et al. (49) used factor analysis to identify modes of MU control during isometric tasks, demonstrating network-level synergies across agonist muscles. Although these results provided valuable insights into overarching neural strategies, they did not address the task-specific differences in shared neural input that can emerge during dynamic conditions such as postural leaning. PCI, on the other hand, bypasses assumptions related to dimensionality reduction and focuses explicitly on the coherence-derived relationships between MU subgroups, offering mechanistic insights into the degree of shared neural input.

Limitations

The methodological approach in this study has limitations, which we have taken steps to mitigate. A potential limitation is the effect of small electrode movements relative to the underlying muscle fibers during different leaning directions. Although participants were instructed to maintain a rigid body posture to minimize these shifts, minor changes in ankle joint angles during leaning tasks could have caused slight displacements of the recording grids. However, it has been shown that changes in ankle joint angles are associated with very small (10 μm) fiber length changes (28) and would have minimal effects on the recording and decomposition results. Furthermore, we used an MU matching threshold of 10% to ensure that slight changes in the waveform would be captured by the algorithm, in addition to matches being visually confirmed by an expert operator.

The accuracy of PCI calculations is influenced by the number of MUs available for analysis. Negro et al. (16) demonstrated that while PCI can be calculated with a minimal number of MU pairs (e.g., two pairs), accuracy improves with a larger MU yield. In our study, PCI was calculated using a standardized minimum number of pairs (i.e., 4 pairs) to ensure methodological consistency across participants and conditions. Furthermore, in our study, PCI was not influenced by motor unit discharge rate.

Finally, we took multiple steps to minimize cross talk from adjacent muscles, including ultrasound-guided placement of HDsEMG grids to ensure precise targeting of the triceps surae, using separate grids for each muscle to reduce signal contamination, selecting interelectrode distances of 10 mm, and assessing single-differential EMG samples to ensure the highest sensitivity (51, 52). These precautions reduce the likelihood that methodological artifacts explain the observed PCI differences.

Conclusions

This study provides evidence for different amounts of shared excitatory synaptic input to distinct MU subgroups within the triceps surae muscles. Furthermore, the amount of common input is related to movement directions and muscle types. Future studies using direct cortical mapping could help further elucidate the structure of these input systems. Complementary methods such as non-negative matrix factorization or principal component analysis may help reveal low-dimensional input modes that better characterize the independence or overlap of control signals across MU subgroups.

DATA AVAILABILITY

Data will be made available to any reasonable request.

GRANTS

This work was supported by the Natural Sciences and Engineering Research Council of Canada: NSERC RGPIN 105424-12.

DISCLOSURES

No conflicts of interest, financial or otherwise, are declared by the authors.

AUTHOR CONTRIBUTIONS

J.W.C. conceived and designed research; J.W.C. performed experiments; J.W.C. analyzed data; J.W.C., T.V., T.D.I., and S.J.G. interpreted results of experiments; J.W.C., T.V., and T.D.I. prepared figures; J.W.C. drafted manuscript; J.W.C., T.V., T.D.I., and S.J.G. edited and revised manuscript; J.W.C., T.V., T.D.I., and S.J.G. approved final version of manuscript.

REFERENCES

1. **Ting LH**, **McKay JL.** Neuromechanics of muscle synergies for posture and movement. *Curr Opin Neurobiol* 17: 622–628, 2007. doi:10.1016/j.conb.2008.01.002.
2. **Bernstein N.** *The Coordination and Regulation of Movements*. Pergamon Press, 1967.
3. **Klein Breteler MD**, **Simura KJ**, **Flanders M.** Timing of muscle activation in a hand movement sequence. *Cereb Cortex* 17: 803–815, 2007. doi:10.1093/cercor/bhk033.
4. **Tresch MC**, **Saltiel P**, **Bizzi E.** The construction of movement by the spinal cord. *Nat Neurosci* 2: 162–167, 1999. doi:10.1038/5721.
5. **Torres-Oviedo G**, **Macpherson JM**, **Ting LH.** Muscle synergy organization is robust across a variety of postural perturbations. *J Neurophysiol* 96: 1530–1546, 2006. doi:10.1152/jn.00810.2005.
6. **Torres-Oviedo G**, **Ting LH.** Muscle synergies characterizing human postural responses. *J Neurophysiol* 98: 2144–2156, 2007. doi:10.1152/jn.01360.2006.

7. **d'Avella A**, **Portone A**, **Fernandez L**, **Lacquaniti F.** Control of fast-reaching movements by muscle synergy combinations. *J Neurosci* 26: 7791–7810, 2006. doi:10.1523/JNEUROSCI.0830-06.2006.
8. **Flash T**, **Hochner B.** Motor primitives in vertebrates and invertebrates. *Curr Opin Neurobiol* 15: 660–666, 2005. doi:10.1016/j.conb.2005.10.011.
9. **Hug F**, **Del Vecchio A**, **Avrillon S**, **Farina D**, **Tucker K.** Muscles from the same muscle group do not necessarily share common drive: evidence from the human triceps surae. *J Appl Physiol (1985)* 130: 342–354, 2021. doi:10.1152/japplphysiol.00635.2020.
10. **Formento E**, **Botros P**, **Carmena J.** Skilled independent control of individual MUs via a non-invasive neuromuscular–machine interface. *J Neural Eng* 18: 10.1088/1741–12552/ac35ac, 2021. doi:10.1088/1741-2552/ac35ac.
11. **Hug F**, **Avrillon S**, **Ibanez J**, **Farina D.** Common synaptic input, synergies and size principle: Control of spinal motor neurons for movement generation. *J Physiol* 601: 11–20, 2023. doi:10.1113/JP283698.
12. **Bremner F**, **Baker J**, **Stephens J.** Correlation between the discharges of MUs recorded from the same and from different finger muscles in man. *J Physiol* 432: 355–380, 1991. doi:10.1113/jphysiol.1991.sp018389.
13. **Gibbs J**, **Harrison LM**, **Stephens JA.** Organization of inputs to motoneurone pools in man. *J Physiol* 485: 245–256, 1995. doi:10.1113/jphysiol.1995.sp020727.
14. **Kerkman JN**, **Daffertshofer A**, **Gollo LL**, **Breakspear M**, **Boonstra TW.** Network structure of the human musculoskeletal system shapes neural interactions on multiple time scales. *Sci Adv* 4: eaat0497, 2018. doi:10.1126/sciadv.aat0497.
15. **Laine CM**, **Martinez-Valdes E**, **Falla D**, **Mayer F**, **Farina D.** Motor neuron pools of synergistic thigh muscles share most of their synaptic input. *J Neurosci* 35: 12207–12216, 2015. doi:10.1523/JNEUROSCI.0240-15.2015.
16. **Negro F**, **Yavuz US**, **Farina D.** The human motor neuron pools receive a dominant slow-varying common synaptic input. *J Physiol* 594: 5491–5505, 2016. doi:10.1113/JP271748.
17. **Del Vecchio A**, **Germer C**, **Elias L**, **Fu Q**, **Fine J**, **Santello M**, **Farina D.** The human central nervous system transmits common synaptic inputs to distinct motor neuron pools during non-synergistic digit actions. *J Physiol* 597: 5935–5948, 2019. doi:10.1113/JP278623.
18. **Cohen JW**, **Vieira T**, **Ivanova TD**, **Cerone GL**, **Garland SJ.** Maintenance of standing posture during multi-directional leaning demands the recruitment of task-specific MUs in the ankle plantarflexors. *Exp Brain Res* 239: 2569–2581, 2021. doi:10.1007/s00221-021-06154-0.
19. **Cohen JW**, **Vieira T**, **Ivanova TD**, **Garland SJ.** Differential behaviour of distinct motoneuron pools that innervate the triceps surae. *J Neurophysiol* 129: 272–284, 2023. doi:10.1152/jn.00336.2022.
20. **Cohen JW**, **Vieira TM**, **Ivanova TD**, **Garland SJ.** Regional recruitment and differential behavior of MUs during postural control in older adults. *J Neurophysiol* 130: 1321–1333, 2023. doi:10.1152/jn.00068.2023.
21. **Semmler JG**, **Kornatz KW**, **Enoka RM.** Motor-unit coherence during isometric contractions is greater in a hand muscle of older adults. *J Neurophysiol* 90: 1346–1349, 2003. doi:10.1152/jn.00941.2002.
22. **Jaiser SR**, **Baker MR**, **Baker SN.** Intermuscular coherence in normal adults: variability and changes with age. *PLoS One* 11: e0149029, 2016. doi:10.1371/journal.pone.0149029.
23. **Negro F**, **Muceli S**, **Castronovo AM**, **Holobar A**, **Farina D.** Multichannel intramuscular and surface EMG decomposition by convolutive blind source separation. *J Neural Eng* 13: 026027, 2016. doi:10.1088/1741-2560/13/2/026027.
24. **Scaglioni G**, **Narici MV**, **Maffiuletti NA**, **Pensini M**, **Martin A.** Effect of ageing on the electrical and mechanical properties of human soleus MUs activated by the H reflex and M wave. *J Physiol* 548: 649–661, 2003. doi:10.1113/jphysiol.2002.032763.
25. **Farina D**, **Negro F.** Common synaptic input to motor neurons, MU synchronization, and force control. *Exerc Sport Sci Rev* 43: 23–33, 2015. doi:10.1249/JES.0000000000000032.
26. **Thomsen MH**, **Stottrup N**, **Larsen FG**, **Pedersen ASK**, **Poulsen AG**, **Hirata RP.** Four-way-leaning test shows larger limits of stability than a circular-leaning test. *Gait Posture* 51: 10–13, 2017. doi:10.1016/j.gaitpost.2016.09.018.
27. **Morasso PG**, **Sanguineti V.** Ankle muscle stiffness alone cannot stabilize balance during quiet standing. *J Neurophysiol* 88: 2157–2162, 2002. doi:10.1152/jn.2002.88.4.2157.
28. **Loram ID**, **Maganaris CN**, **Lakie M.** Human postural sway results from frequent, ballistic bias impulses by soleus and gastrocnemius. *J Physiol* 564: 295–311, 2005. doi:10.1113/jphysiol.2004.076307.
29. **Holobar A**, **Minetto M**, **Botter A**, **Farina D.** *Identification of MU Discharge Patterns from High-Density Surface EMG during High Contraction Levels*. Springer, 2011, p. 1165–1168.
30. **Holobar A**, **Farina D.** Blind source identification from the multichannel surface electromyogram. *Physiol Meas* 35: R143–R165, 2014. doi:10.1088/0967-3334/35/7/R143.
31. **Power KE**, **Lockyer EJ**, **Botter A**, **Vieira T**, **Button DC.** Endurance-exercise training adaptations in spinal motoneurones: potential functional relevance to locomotor output and assessment in humans. *Eur J Appl Physiol* 122: 1367–1381, 2022. doi:10.1007/s00421-022-04918-2.
32. **Farina D**, **Merletti R**, **Enoka RM.** The extraction of neural strategies from the surface EMG: an update. *J Appl Physiol (1985)* 117: 1215–1230, 2014. doi:10.1152/japplphysiol.00162.2014.
33. **Farina D**, **Negro F**, **Gazzoni M**, **Enoka RM.** Detecting the unique representation of motor-unit action potentials in the surface electromyogram. *J Neurophysiol* 100: 1223–1233, 2008. doi:10.1152/jn.90219.2008.
34. **De Luca CJ**, **Erim Z.** Common drive of MUs in regulation of muscle force. *Trends Neurosci* 17: 299–305, 1994. doi:10.1016/0166-2236(94)90064-7.
35. **De Luca CJ**, **Erim Z.** Common drive in MUs of a synergistic muscle pair. *J Neurophysiol* 87: 2200–2204, 2002. doi:10.1152/jn.00793.2001.
36. **Semmler JG**, **Nordstrom MA**, **Wallace CJ.** Relationship between MU short-term synchronization and common drive in human first dorsal interosseous muscle. *Brain Res* 767: 314–320, 1997. doi:10.1016/s0006-8993(97)00621-5.
37. **Mochizuki G**, **Semmler JG**, **Ivanova T**, **Garland S.** Low-frequency common modulation of soleus MU discharge is enhanced during postural control in humans. *Exp Brain Res* 175: 584–595, 2006. doi:10.1007/s00221-006-0575-7.
38. **Farina D**, **Jiang N**, **Rehbaum H**, **Holobar A**, **Graimann B**, **Dietl H**, **Aszmann OC.** The extraction of neural information from the surface EMG for the control of upper-limb prostheses: emerging avenues and challenges. *IEEE Trans Neural Syst Rehabil Eng* 22: 797–809, 2014. doi:10.1109/TNSRE.2014.2305111.
39. **Negro F**, **Farina D.** Factors influencing the estimates of correlation between MU activities in humans. *PLoS One* 7: e44894, 2012. doi:10.1371/journal.pone.0044894.
40. **Desmedt HE**, **Godaux E.** Spinal motoneuron recruitment in man: rank deordering with direction but not with speed of voluntary movement. *Science* 214: 933–936, 1981. doi:10.1126/science.7302570.
41. **Cohen JW**, **Gallina A**, **Ivanova TD**, **Vieira T**, **McAndrew DJ**, **Garland SJ.** Regional modulation of the ankle plantarflexor muscles associated with standing external perturbations across different directions. *Exp Brain Res* 238: 39–50, 2020. doi:10.1007/s00221-019-05696-8.
42. **Dean JC.** Proprioceptive feedback and preferred patterns of human movement. *Exerc Sport Sci Rev* 41: 36–43, 2013. doi:10.1097/JES.0b013e3182724bb0.
43. **Jacobs JV**, **Horak FB.** Cortical control of postural responses. *J Neural Transm (Vienna)* 114: 1339–1348, 2007. doi:10.1007/s00702-007-0657-0.
44. **Buchanan TS**, **Lloyd DG.** Muscle activity is different for humans performing static tasks which require force control and position control. *Neurosci Lett* 194: 61–64, 1995. doi:10.1016/0304-3940(95)11727-e.
45. **Spiliopoulou S**, **Amiridis IG**, **Hatzitaki V**, **Patikas D**, **Kellis E.** Tendon vibration during submaximal isometric strength and postural tasks. *Eur J Appl Physiol* 112: 3807–3817, 2012. doi:10.1007/s00421-012-2319-7.
46. **De Luca CJ**, **LeFever RS**, **McCue MP**, **Xenakis AP.** Control scheme governing concurrently active human MUs during voluntary contractions. *J Physiol* 329: 129–142, 1982. doi:10.1113/jphysiol.1982.sp014294.
47. **Taylor AM**, **Enoka RM.** Optimization of input patterns and neuronal properties to evoke motor neuron synchronization. *J Comput Neurosci* 16: 139–157, 2004. doi:10.1023/B:JCNS.0000014107.16610.2e.

48. **Keen DA**, **Chou LW**, **Nordstrom MA**, **Fuglevand AJ.** Short-term synchrony in diverse motor nuclei presumed to receive different extents of direct cortical input. *J Neurophysiol* 108: 3264–3275, 2012. doi:10.1152/jn.01154.2011.
49. **Del Vecchio A**, **Germer CM**, **Kinfe TM**, **Nuccio S**, **Hug F**, **Eskofier B**, **Farina D**, **Enoka RM.** The forces generated by agonist muscles during isometric contractions arise from MU synergies. *J Neurosci* 43: 2860–2873, 2023. doi:10.1523/JNEUROSCI.1265-22.2023.
50. **Weinman LE**, **Del Vecchio A**, **Mazzo MR**, **Enoka RM.** MU modes in the calf muscles during a submaximal isometric contraction are changed by brief stretches. *J Physiol* 602: 1385–1404, 2024. doi:10.1113/JP285437.
51. **Vieira TM**, **Botter A**, **Muceli S**, **Farina D.** Specificity of surface EMG recordings for gastrocnemius during upright standing. *Sci Rep* 7: 13300, 2017. doi:10.1038/s41598-017-13369-1.
52. **Vieira TM**, **Cerone GL**, **Botter A**, **Watanabe K**, **Vigotsky AD.** The sensitivity of bipolar electromyograms to muscle excitation scales with the inter-electrode distance. *IEEE Trans Neural Syst Rehabil Eng* 31: 4245–4255, 2023. doi:10.1109/TNSRE.2023.3325132.